Populations of High Energy Sources in Galaxies
Proceedings IAU Symposium No. 230, 2005
E. J. A. Meurs & G. Fabbiano, eds.

doi:10.1017/S1743921306008787

Models for the Evolution of X-Ray Binaries in a Young Stellar Population

M. Eracleous[1], M. S. Sipior[2], and S. Sigurdsson[1]

[1]Department of Astronomy & Astrophysics, The Pennsylvania State Univeristy, 525 Davey Lab, University Park, PA 16802, USA

[2]Astronomical Institute "Anton Pannekoek" and Section Computational Sciences, University of Amsterdam, Kruislaan 403, 1098 SJ, Amsterdam, The Netherlands

Abstract. We present the results of population synthesis simulations aimed at exploring the evolution of the 2–10 keV luminosity of X-ray binaries in a young stellar population. The results are applicable to populations of extragalactic X-ray binaries in starburst galaxies and many LINERs. We find that the integrated 2–10 keV luminosity of the simulated population reaches a maximum of about 10^{40} erg s^{-1} after approximately 20 Myr (for a star-formation rate of 10 M$_\odot$ yr^{-1}) and remains significant even after the end of star formation and the demise of the luminous OB stars. The results of our simulation are in agreement with recently-derived correlations between the X-ray luminosity starburst galaxies and their star-formation rate. We also find that the cumulative luminosity function is initially fairly flat, in agreement with recent observational results, becoming steeper as the population ages and the high-mass X-ray binaries are succeeded by binaries with progressively lighter donor stars. Using the output of Hydrogen-ionizing far-UV photons from the stellar population, we can plot the track of a "post-starburst" system in the $L_{\rm X} - L_{\rm H\alpha}$ diagram. The system starts off in the starburst locus but quickly evolves to the AGN locus where it lingers for at least 1 Gyr.

1. Introduction

With the advent of of the *Chandra* X-ray observatory, we can resolve populations of discrete X-ray sources (presumably X-ray binaries; hereafter XRBs) in many galaxies other than our own. Thus, we have been able to confirm and extend previously known differences (e.g., Fabbiano 1995; Fabbiano & White 2005) between the XRB populations of old and young stellar systems (steeper luminosity functions in the former compared to the latter; e.g., Eracleous *et al.* 2002; Colbert *et al.* 2004). We have also been able to establish correlations between the star formation rate and the 2–10 keV X-ray luminosity of a star-forming galaxy (e.g., Ranalli *et al.* 2003; Grimm *et al.* 2002; Colbert *et al.* 2004; Persic *et al.* 2004).

To understand the origin of these observational properties of galaxies and to predict the evolution of star-forming systems, we have undertaken a theoretical investigation of the evolution of X-ray binaries formed in a brief star-formation episode. The results of this investigation should also be useful in interpreting the properties of distant star-forming galaxies found in deep X-ray surveys (e.g., Bauer *et al.* 2004).

2. Population Synthesis Simulations: Code and Methods

We have carried out simulations of the early evolution of XRBs formed in a burst of star formation, using a modified version of the Monte-Carlo population synthesis code of Pols & Marinus (1994). This code was modified initially by Bloom *et al.* (1999) to include supernova kicks. It was later extended by Sipior & Sigurdsson (2002) to include a mapping of the initial star mass to a final black hole mass, and thus account for evolution to the black hole state. Sipior (2003) made considerable refinements to the treatment of mass transfer by adopting the methodology of Hurley *et al.* (2002) and implementing duty cycles due to accretion disk instabilities and X-ray attenuation by circumstellar material. The code was further upgraded to use the massive main sequence star models of Meynet & Maeder (2003), which include rotation and mass loss self consistently (via the formalism of Nugis & Lamers 2000). The main output of a simulation consists of an evolutionary record for each binary, which can be used as the stepping stone for computing the total luminosity of the population and the luminosity function.

The total X-ray luminosity of the population versus time is computed by summing the contributions from all XRBs weighted by the appropriate efficiency factors, namely

$$L_{2-10\ \rm keV}\ (t) \ = \sum_{\text{all XRBs at } t} \eta_{st}\ \eta_x\ \eta_{bol}\ \eta_a\ L_{bol}, \tag{2.1}$$

where L_{bol} is the total available accretion power. The preceding terms are efficiency factors, as follows: η_{st} is the duty cycle due to accretion disk instabilities, which depends on the period the type of compact object, and the relative mass of the companion (see Li & Wang 1998; King 2001); η_{bol} is the fraction of the available accretion power converted to radiation (assumed to be 0.5 for black holes and 1.0 for neutron stars); η_x is the fraction of the radiated power emerging in the 2–10 keV band (assumed to be 0.4 for black holes and 0.2 for neutron stars); η_a is the attenuation factor due to photoelectric absorption in circumstellar material (the column density is computed by assuming that material lost from the binary forms a spherical shell around it).

3. Application and Results

Our simulation considers a star formation episode with a constant star-formation rate (SFR) of 10 $M_\odot$ yr^{-1} and a duration of 20 Myr. The main result, depicted in Figure 1, is the evolution of the total luminosity of the system with time for 2 Gyr. As expected, the black hole XRBs (whose companions are typically massive) turn on very early and remain active as long as the star-formation continues. They track the star-formation episode (and rate) fairly closely and they disappear very soon after the end of star formation. In contrast, the neutron star XRBs (whose companions are typically less massive) turn on with a delay and persist for a longer time. This is a consequence of the lower mass of their companions and the fact that different generations of systems with progressively lighter companions turn on with progressively longer delays. As a result, the total luminosity of the system remains appreciable up to almost 1 Gyr after the end of star formation. The rate of decline of the total luminosity from all flavors of XRBs, after the end of star formation, is approximately $\propto t^{-1.4}$.

These results are insensitive to the assumed initial mass function (IMF) and distribution of binary mass ratios (q-distribution); combinations of the Salpeter and Miller-Scalo IMFs with flat and low-skewed q-distributions yield nearly identical results. On the other hand, the assumed distribution of supernova kicks has a significant effect on the resulting X-ray luminosity. Our adopted kick distribution is a Gaussian with a dispersion of 90 km s^{-1}; increasing this dispersion to 190 and 450 km s^{-1} reduces the number of XRBs by factors of 1.6 and 2.6 respectively.

The total luminosity from black hole XRBs appears to reach a steady state at about 10 Myr after the beginning of the star-formation episode. The luminosity of this plateau is $L_X \approx 1 \times 10^{40}$ erg s^{-1}, which is consistent with the empirically determined correlations

https://doi.org/10.1017/S1743921306008787 Published online by Cambridge University Press

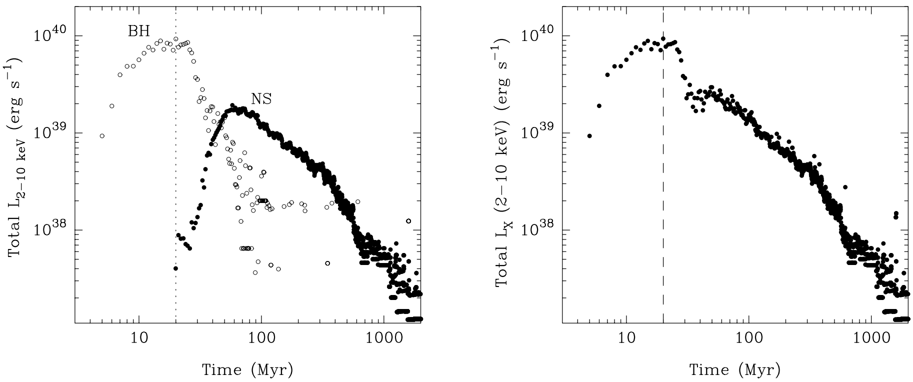

Figure 1. The evolution of the total X-ray luminosity from XRBs formed in an episode of star formation with SFR = 10 $M_\odot$ yr^{-1} and duration 20 Myr. The end of the star-formation episode is marked by a vertical dashed line. The left panel shows the separate contributions from black hole XRBs (open circles) and neutron star XRBs (filled circles). The panel on the right shows the evolution of the total luminosity from all of XRBs. Notice the delay in the onset of the NS XRBs, which causes the X-ray luminosity to remain high long after the end of star formation. The results presented here are for a Salpeter IMF and a low-skewed q-distribution.

between L_X and the SFR (empirically, we expect L_X in the range $4\times10^{39}-7\times10^{40}$ erg s^{-1} for our assumed SFR). The cumulative luminosity function [CLF, $N(>L) \propto L^{-\beta}$] is quite flat while the star formation episode is in progress. After the episode is over the CLF becomes steeper with $\beta \sim 0.5$, 1.0, and 1.3 at a time of 20, 30, and 40 Myr after the end of star formation, respectively (with a some variation in β with assumed IMF and q-distribution). In comparison, the observed values of β for star-forming galaxies are in the range 0.5–1.0 (e.g., Grimm *et al.* 2002; Colbert *et al.* 2004).

4. Discussion

An important conclusion from our simulations is that the X-ray luminosity of a "post-starburst" system can remain high up to 1 Gyr after the end of star formation and the demise of the luminous OB stars. The LINER NGC 4736 (Eracleous *et al.* 2002) may be an example of such a system. In this spirit, we can attempt to follow the evolution of a post-starburst system in the $L_X - L_{\mathrm{H}\alpha}$ diagram, which has been used as a tool for discriminating between nuclear and starburst activity (e.g., Ho *et al.* 2001). The key physical effect that determines the track of a post-starburst system in this diagram is the different rates of decline of the X-ray and Hα luminosities after the end of star formation; the former declines as $t^{-1.4}$, while the latter declines much more quickly, as t^{-4} to t^{-5} (Binette *et al.* 1994; Sternberg *et al.* 2003). The rapid decline in the Hα luminosity is a direct consequence of the short life times of OB stars, which provide the vast majority of Hydrogen-ionizing photons. At very late times ($t \sim 60 - 100$ Myr), the Hα emission is driven by ionizing photons from the old stellar population (post-AGB stars and nuclei of PNe, see Binette *et al.* 1994), leading to $L_{\mathrm{H}\alpha} \propto t^{-0.6}$.

In Figure 2 we plot the track of a post-starburst system in the $L_X - L_{\mathrm{H}\alpha}$ diagram, under the scenario outlined above. The system starts in the starburst galaxy locus but it evolves very quickly to the AGN locus, where it appears to linger for at least 1 Gyr. Thus a post-starburst system at the late stages of its evolution could be mistaken for a low-luminosity AGN since it has a similar X-ray luminosity and very likely also a similar X-ray spectrum. The best way to to avoid this confusion is to use high-resolution

https://doi.org/10.1017/S1743921306008787 Published online by Cambridge University Press

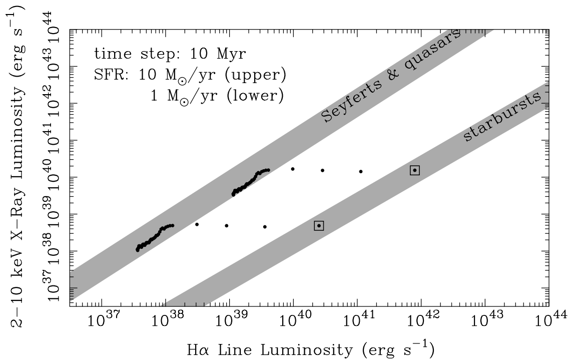

Figure 2. The evolution of a simulated population in the $L_X - L_{\mathrm{H}\alpha}$ diagram. At the end of star formation the system is in the starburst galaxy locus (location indicated by ◙). As the population ages, the system moves to the left along the dotted track at a rate of 10 Myr per dot. The initial evolution is very rapid because the Hα luminosity drops precipitously with the demise of the OB stars. After 40–50 Myr the evolution slows down and the system lingers in the AGN locus for at least 1 Gyr. The tracks shown here correspond to SFR values of 1 and 10 $M_\odot$ yr^{-1}, and under the assumption of a Salpeter IMF and a low-skewed q distribution.

X-ray images, such as those provided by *Chandra*, which can resolve the individual XRBs contributing to the total X-ray luminosity.

Acknowledgements

This work was supported by NASA through grant GO0-1152A,B from the Smithsonian Astrophysical Observatory, from NSF grant PHY-0203046, and from the Center for Gravitational Wave Physics, which is supported by the NSF under cooperative agreement PHY 01-14375.

References

Bauer, F. E., *et al.* 2004, AJ, 128, 2048
Binette, L., Magris, C. G, Stasińska, G., & Bruzual, A. G. 1994, A&A, 192, 13
Bloom, J. S., Sigurdsson, S., & Pols, O. R. 1999, MNRAS, 305, 763
Colbert, E., *et al.* 2004, ApJ, 602, 231
Eracleous, M., Shields, J. C., Chartas, G., & Moran, E. C. 2002, ApJ, 565, 108.
Fabbiano, G. 1995 in *X-Ray Binaries*, eds, W. H. G. Lewin, *et al.* (Cambridge U. Press), 390
Fabbiano, G. & White, N. E. in *Compact Stellar X-ray Sources*, eds, W. H. G. Lewin & M. van der Klis (Cambridge U. Press), in press (astro-ph/0307077)
Grimm, H.-J., Gilfanov, M., & Sunyaev, R. 2002, MNRAS, 339, 793
Ho, L. C., *et al.* 2001, ApJ, 549, L51
Hurley, J. R., Tout, C. A., & Pols, O. R. 2002, MNRAS, 329, 897
King, A. R. 2001, in Black Holes in Binaries and Galactic Nuclei, eds. L. Kaper, E. P. J. van den Heuvel, & P. A. Woudt (ESO Workshop), 155
Li, X.-D., & Wang, Z.-R. 1998, ApJ, 500, 935
Meynet, G. & Maeder, A. 2003, A&A, 404, 975
Nugis, T. & Lamers, H. J. G. L. M. 2000, A&A, 360, 227
Persic, M., *et al.* 2004, A&A, 419, 849
Pols, O. R. & Marinus, M. 1994, A&A, 288, 475
Ranalli, P., Comastri, A., & Setti, G. 2003, A&A, 399, 39
Sternberg, A., Hoffmann, T. L., & Pauldrach, A. W. A. 2003, ApJ, 599, 1333
Sipior, M. S. 2003, Ph. D. Thesis, The Pennsylvania State University
Sipior, M. S. & Sigurdsson, S. 2002, ApJ, 572, 962

Discussion

IVANOVA: Can you comment on what is the role of thermally unstable MT and how do you calculate this?

ERACLEOUS: We do not use a sophisticated treatment of mass transfer in the thermally unstable case. We just assume that the entire envelope mass of the donor is lost on the thermal time scale. This is a very high mass transfer rate, but a large fraction of the matter lost from the secondary escapes from the system. In this case we assume that the escaping material attenuates the emitted X-rays, so these systems can be very dim and do not affect the total X-ray luminosity of the population.

ZEZAS: How do the results depend on the choice of the IMF?

ERACLEOUS: The results are not sensitive to the choice of IMF. We have carried out the simulation using both a Salpeter IMF and a Miller-Scalo IMF and we get almost indistinguishable results.

LIPUNOV: Please in the future give the comparison with previous results.

ERACLEOUS: Thanks, that is a good suggestion. I have not compared with old results, but I have compared with with very recent results, specifically those by VanBever and Vanbeveren (2000); we are in good agreement.

The speaker sampling some Irish culture. Photo courtesy of M. Eracleous.

https://doi.org/10.1017/S1743921306008787 Published online by Cambridge University Press

Michael Garcia in stead of Michael Eracleous (see previous photograph). Photo courtesy of M. Eracleous.

https://doi.org/10.1017/S1743921306008787 Published online by Cambridge University Press